General digital microfluidic platform manipulating dielectric and conductive droplets by dielectrophoresis and electrowetting†

Shih-Kang Fan,* Tsung-Han Hsieh and Di-Yu Lin

Received 24th September 2008, Accepted 9th January 2009
First published as an Advance Article on the web 16th February 2009
DOI: 10.1039/b816535a

A general digital (droplet-based) microfluidic platform based on the study of dielectric droplet manipulation by dielectrophoresis (DEP) and the integration of DEP and electrowetting-on-dielectric (EWOD) is reported. Transporting, splitting, and merging dielectric droplets are achieved by DEP in a parallel-plate device, which expands the fluids of digital microfluidics from merely being conductive and aqueous to being non-conductive. In this work, decane, hexadecane, and silicone oil droplets were successfully transported in a 150 μm-high gap between two parallel plates by applying a DC voltage above threshold voltages. Non-volatile silicone oil droplets with viscosities of 20 and 50 cSt were studied in more detail in parallel-plate geometries with spacings of 75 μm, 150 μm, and 225 μm. The threshold voltages and the required driving voltages to achieve droplet velocities up to 4 mm/s in the different circumstances were measured. By adding a dielectric layer on the driving electrodes of the tested parallel-plate device, a general digital microfluidic platform capable of manipulating both dielectric and conductive droplets was demonstrated. DEP and EWOD, selectively generated by applying different signals on the same dielectric-covered electrodes, were used to drive silicone oil and water droplets, respectively. Concurrent transporting silicone oil and water droplets along an electrode loop, merging water and oil droplets, and transporting and separating the merged water-in-oil droplet were performed.

Introduction

Liquid droplet manipulation has been extensively studied for a wide variety of applications. First, a droplet can be thought of as an independent liquid compartment where chemical or biological syntheses can take place[1–3] and used with lab-on-a-chip (LOC) technology. Basic digital (droplet-based) microfluidic functions have been demonstrated by creating, transporting, splitting, and merging droplets between parallel plates.[4] Second, in addition to serving as microreactors, the diversity of available droplet materials has led to optical, electrical, and thermal applications commensurate with their appropriate physical properties. For example, droplet-based lenses[5,6] and mirrors[7] have been fabricated by controlling the surface profile or the position of a droplet with the proper refractive index. Similarly, the electrical or thermal properties can be used to make droplets that are able to conduct current[8] or heat.[9,10] In the above applications, conductive and aqueous droplets are individually manipulated by electrical means, including electrostatic forces,[1] dielectrophoresis (DEP),[2,3] and electrowetting-on-dielectric (EWOD).[4–10] Because electrical pumping relies on the electric properties of the liquid, actuating non-conductive, or dielectric, droplets has rarely been reported, not to mention the manipulation of both conductive and dielectric droplets on a single device.

However, both conductive and dielectric droplets are equally important from the viewpoint of their potential applications. In the LOC applications, the ability to handle dielectric droplets enables reactions involving non-conductive organic solutions. In the applications taking advantage of the droplets' inherent physical properties, dielectric droplets would provide similar but more stable functions free from evaporation and electrolysis. In this paper, we first demonstrate repeatable dielectric droplet manipulations through DEP. This technique is further integrated with EWOD to realize a general digital microfluidic platform capable of actuating droplets with different conductivities and polarities. For example, by sequentially transporting lipid-dissolved decane or hexadecane droplets (dielectric and nonpolar) and electrolyte droplets (conductive and polar) through an aperture, an artificial lipid bilayer membrane could be formed, as it has been previously demonstrated in microchannels where liquids were pumped mechanically.[11]

Principle

As mentioned above,[4–10] EWOD has been widely used to manipulate conductive droplets by modulating its contact angle through voltage application across a dielectric layer.[12] However, driving dielectric droplets, *e.g.*, decane, by EWOD was not successful.[13] Another extensively studied driving force of droplets, DEP,[14] has been known for its manipulation of polarizable

Institute of Nanotechnology, National Chiao Tung University, 207, Engineering 1, 1001 University Road, Hsinchu, Taiwan. E-mail: skfan@mail.nctu.edu.tw; Fax: +886-3-5729912; Tel: +886-3-5712121 ext 55813

† Electronic supplementary information (ESI) available: Threshold and splitting voltages (Table s1); velocities plotted against DEP forces (Fig. s1); derivation of the Maxwell stress tensor; video of silicone oil manipulation (Video 1); video of concurrent oil and water droplet pumping (Video 2); video of merging droplets and transporting the merged droplet by EWOD (Video 3); and video of separating the merged droplet (Video 4). See DOI: 10.1039/b816535a

particles, including nucleic acids, proteins, cells, and nanoparticles, by non-uniform electric fields in liquids.[15–17] When considering liquid droplets as suspended objects, individual droplets were successfully driven by DEP in immiscible fluid media.[2,3,18] Droplet-based LOC where water droplets were driven by DEP in immiscible 1-bromododecane was demonstrated.[3] Because DEP was regarded as a body force exerting on the whole droplets, splitting droplets were not performed.

In addition to providing body forces on suspended objects of interest, drawing bulk dielectric liquids of higher relative permittivity (liquid) into a strong electric field region of lower relative permittivity (air) was also demonstrated.[15,19–22] Over 100 years ago, rising dielectric liquid by applying a DC voltage between a pair of electrode plates dipped vertically into a dish full of the dielectric liquid was achieved by macroscopic apparatus.[19] The height-of-rise was experimentally and theoretically explained by force balance between the gravity force and the DEP force (F_{DEP}) in the direction normal to the surface acting from the dielectric liquid to air. By applying V between W-wide parallel electrode plates spaced d apart, F_{DEP} is:

$$F_{DEP} = \frac{\varepsilon_0(\varepsilon - 1)W}{2d}V^2 \quad (1)$$

where ε_0 (8.85×10^{-12} F/m) is the permittivity of vacuum, and ε is the relative permittivity of the liquid. The phenomenon was applied to orient cryogenic liquids under near zero-gravity conditions.[20–22]

More recently, similar to dielectric liquids, aqueous liquids were drawn against gravity by an AC electric field between parallel electrode plates coated with dielectric layers.[23,24] A dielectric layer was used to prevent electrochemical reactions at the liquid-electrode interfaces, and AC signals were chosen to make the signal to penetrate the dielectric layer and generate voltage across the liquid. Furthermore, formation of aqueous liquid columns and droplets on an open surface by DEP through dielectric-coated coplanar electrode patterns were demonstrated.[25,26]

Here we combine vertical rising of bulk dielectric liquids between electrodes and horizontal transporting of droplets by bottom electrodes to realize dielectric droplet manipulations, including transporting, splitting, and merging, in a parallel-plate device by DEP. As illustrated in Fig. 1(a), when voltage is applied between electrodes, the dielectric droplet would be attracted toward the strong electric field region by DEP. The DEP force exerting on the dielectric droplet by applying V between two W-wide and d-spaced electrodes can be expressed by eqn (1).

Experiments

Device design and fabrication (dielectric droplets)

In addition to merely drawing a dielectric droplet between electrodes (Fig. 1(a)), to achieve replicable digital microfluidic functions, a parallel-plate device was designed to manipulate dielectric droplets by DEP as shown in Fig. 1(b). Multiple driving electrodes (shown as five squares in Fig. 1(b)) were patterned on the bottom substrate. The top plate contained an unpatterned reference electrode. A layer of low surface energy material was coated on both plates to reduce the interfacial force between the droplets and the solid surfaces, which facilitates reproducible droplet handling and eliminates residues of the dielectric liquids during operations. The gap height, or droplet thickness, (shown d in Fig. 1), was determined by the thickness of the spacer. By applying voltage between the reference electrode and one of the driving electrodes, a dielectric droplet would be pumped onto the energized electrode as the arrow indicates in Fig. 1(b).

The tested devices were fabricated on glass substrates for ideal electric isolation between the patterned driving electrodes and for easier observation of the droplets. For the same observation purposes, the reference electrode on the top plate was made of transparent and conductive ITO (indium tin oxide). A layer of 200 nm-thick ITO was first deposited on the top glass substrate and subsequently covered by a low surface energy material, Teflon. Teflon AF 1600 (DuPont) dissolved in FC-77 (3M) at a concentration of 1 wt.% was spun on the ITO-coated top plate at 3000 rpm for 30 s to prepare a 60 nm-thick Teflon layer. Meanwhile, a layer of 200 nm-thick Cu/Cr or ITO was deposited on the bottom glass substrate. An array of driving electrodes, measuring 1 mm × 1 mm, was patterned by wet chemical etching. A 60 nm-thick Teflon layer was spun on the bottom plate as the top plate. Before testing, a dielectric droplet was dispensed onto the bottom plate, where proper spacers were attached. Device assembly was completed by placing the top plate on the spacers that were used to define the droplet thickness and the gap height between plates. Finally, wires were connected between the device, the control circuits, and a computer.

Actuation of dielectric droplets

Dielectric droplets of decane ($C_{10}H_{22}$, Fluka), hexadecane ($C_{16}H_{34}$, Fluka), and silicone oil ($((CH_3)_3SiO[-SiO(CH_3)_2]_nSi(CH_3)_3$, Dow Corning 200® Fluid) were tested in parallel-plate devices with a gap height of 150 μm. Table 1 lists the related physical properties of the tested dielectric liquids, including relative permittivity, conductivity, viscosity, and surface tension at 25 °C. The contact angles were measured by the sessile drop method. Without the Teflon layer, the tested droplets wet the ITO electrodes at a very low contact angle (< 3° for silicone oil). 0.2 μl droplets were dispensed in 150 μm-high gaps, resulting in 1.2 mm diameter circular contacts (with a contact area of ~1.2 mm^2) on the top and bottom plates. To evaluate the transportation of different dielectric droplets, the minimum driving voltage was measured and defined as the threshold voltage listed in Table 1. The droplet velocity at the threshold voltage can be as low as 5 μm/s. The surface tension, contact angle, and contact angle hysteresis provide friction, causing different threshold voltages for different droplets. The polarity of the applied DC voltage has no influence on droplet driving, while AC signals tested up to the frequency of 1 kHz actuated dielectric droplets successfully.

Silicone oil droplet manipulations

Non-volatile silicone oil was studied in more detail to comprehend the DEP actuations without evaporation effects. Moreover, silicone oil is easily accessible and widely applied with well-documented properties. The threshold and splitting voltages (listed in supplementary Table s1 in the ESI†) of 20 cSt and 50 cSt

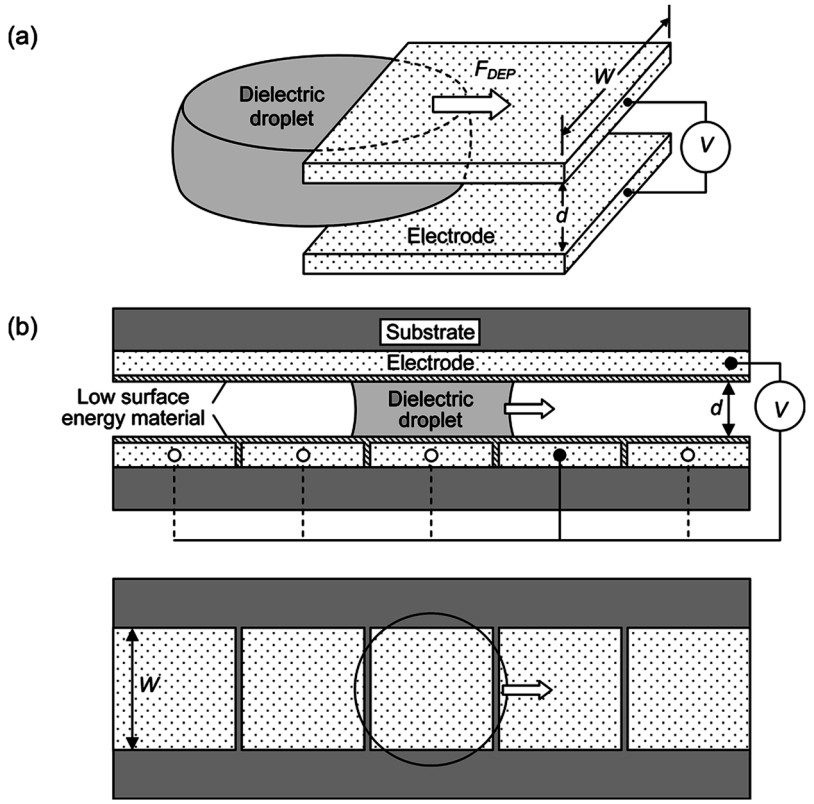

Fig. 1 DEP actuation of dielectric droplets. (a) By applying voltage between parallel electrodes, a liquid dielectric droplet of a higher relative permittivity is pumped by DEP into the region of a lower relative permittivity (*e.g.*, air). (b) Top view and cross section of a parallel-plate device for dielectric droplet manipulations.

silicone oil droplets were measured in 75, 150, and 225 μm-high gaps by 0.1, 0.2, and 0.3 μl droplets, respectively, to maintain a constant contact area of ~1.2 mm^2.

When voltage greater than the threshold voltage was applied, the droplet started to move with a voltage-dependent velocity. The minimum required voltage to drive a droplet following the signal back and forth on the five driving electrodes for at least one cycle at various velocities was recorded and plotted in Fig. 2(a). Each data point represents an averaged voltage from three experiments using different devices. The variation between measurements was within ±10 V. The best-fit quadratic curves indicate that velocity is proportional to the square of the applied voltage, or the DEP force of eqn (1). The velocities are re-plotted against the DEP forces in supplementary Fig. s1 in the ESI,† showing that the velocity is approximately a linear function of the DEP force.

Fig. 2(b)–(g) show the droplet splitting, concurrent double droplet transporting, and merging in a 75 μm-high gap between two plates. For concurrent droplet transporting after splitting, a larger 20 cSt silicone oil droplet (0.15 μl) was used. When voltage (420 V) was applied to the two electrodes neighboring the center one, as indicated by the arrows in Fig. 2(c), the silicone oil droplet started to stretch and neck. The driving electrodes without arrow indications and the reference electrode were electrically grounded. Fig. 2(d) shows two droplets with a similar volume of ~75 nl that were successfully split. The pair of split

Table 1 Properties and threshold voltages of dielectric droplets driven by DEP in a 150 μm-high gap between parallel plates

Liquid	Relative permittivity, ε	Conductivity, σ (S/m)	Viscosity, ν (cSt)	Surface tension, γ (mN/m)	Contact angle on Teflon, θ (degree)	Threshold voltage, V_T (V_{DC})
Decane	1.98[27]	—	0.8[26]	23.3[26]	56.6	350
Hexadecane	2.05[27]	—	3.0[26]	24.9[26]	57.8	470
Silicone oil	2.5[a]	1×10^{-13}[a]	20[a]	20.6[a]	53.2	250

[a] Dow Corning 200® Fluid data sheet.

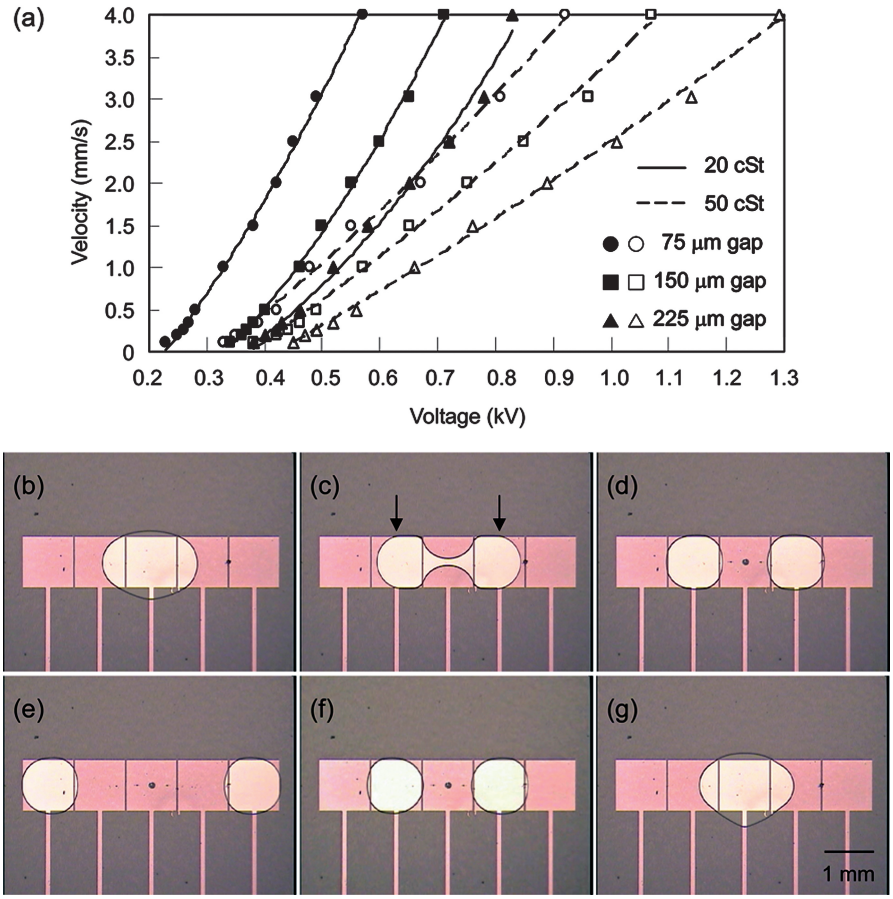

Fig. 2 Digital microfluidic functions of silicone oil droplets. (a) Velocity curves of 20 and 50 cSt silicone oil droplets against voltage in different gap heights: 75, 150, and 225 μm. (b)–(g) Splitting and merging of a 20 cSt silicone oil droplet in a 75 μm-high gap between parallel plates. (b) A 0.15 μl oil droplet was originally positioned on the center electrode. (c) The droplet stretched and necked when 420 V was applied on the two arrow-indicated electrodes. (d) Two ~75 nl oil droplets were successfully split. (e) and (f) Two split droplets were concurrently transported. (g) Split droplets were merged. The supplementary Video 1 can be seen in the ESI.†

droplets was then simultaneously transported in different directions as shown in Fig. 2(e) and (f). The two droplets were then merged into one (Fig. 2(g)).

General digital microfluidic platform

We further tested dielectric droplet manipulation by DEP in a parallel-plate device whose bottom driving electrodes were covered by a dielectric layer, as shown in Fig. 3. For the existence of the dielectric layer, the contact angle of the conductive droplets can be changed from θ_0 to $\theta(V)$ (Fig. 3(a)) by EWOD when applying voltage across the dielectric layer. The dielectric layer used in this study was 1 μm-thick SU-8, prepared by spin coating. Two ~25 nl silicone oil (20 cSt) and water droplets were first placed on the electrode loop consisting of 12 square driving electrodes (1 mm × 1 mm) in a 25 μm-high gap between parallel plates as shown in Fig. 3(b). The top oil droplet was driven to the left through DEP by applying 260 V_{DC} (V_{DEP}) on the left neighboring electrode highlighted by the solid line (Fig. 3(c) and (d)). Concurrently, the bottom water droplet was moved to the right by EWOD when a 34 Vrms and 1 kHz sine wave signal (V_{EWOD}) was applied on the right neighboring electrode indicated by the dashed line. With the same electrodes but different applied signals (V_{DEP} or V_{EWOD}), oil and water droplet were individually and concurrently driven as shown in Fig. 3(d)–(f). The water droplet was then pumped by EWOD toward the oil droplet as can be seen in Fig. 3(f) and (g). After the water droplet touched the oil droplet, it was encompassed by the oil droplet (Fig. 3(h)). The water droplet was pumped across the oil droplet (Fig. 3(i)) as in a filler medium of oil. Furthermore, the water droplet was able to pull the whole merged water-in-oil droplet by EWOD (Fig. 3(j)–(m)), which is similar as the actuation of water-oil core-shell droplets.[28] Finally, as shown in Fig. 3(n)–(p), the merged droplet was separated into water (mostly) and oil droplets by applying EWOD to drive the water droplet and DEP to draw the oil.

Discussions

To pump oil and water droplets efficiently on the general digital microfluidic platform, the driving voltages (V_{DEP} and V_{EWOD}) were different. It is because that the applied voltage should be distributed appropriately (across liquid or dielectric layer) to achieve sufficient driving forces. As indicated by eqn (1), a voltage difference across liquid droplet (V_L in Fig. 4(a)) and between the plates is necessary to drive the oil droplet by DEP. However, EWOD requires a sufficient voltage drop (V_D) across

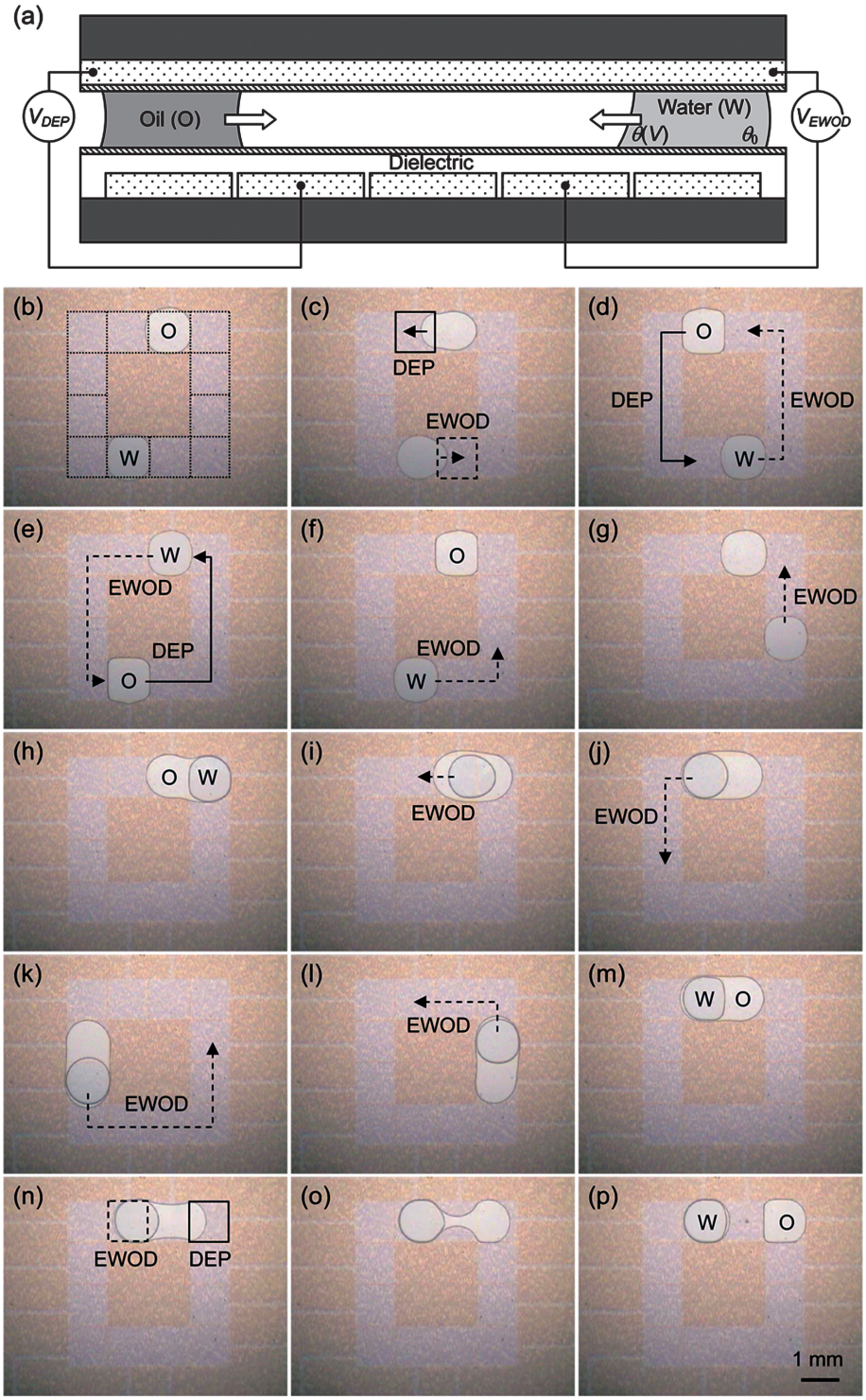

Fig. 3 Manipulating oil and water droplets by DEP and EWOD, respectively, on a parallel-plate device containing a dielectric layer on the bottom plate. (a) Device configuration. Oil and water droplets were driven concurrently by V_{DEP} and V_{EWOD}, respectively. (b) Initial positions of ~25 nl water and oil droplets on a loop of 12 square electrodes (1 mm × 1mm). (c) The oil droplet was pumped to the left by DEP when 260 V_{DC} (V_{DEP}) was applied on the electrode indicated by the solid line. Simultaneously, the water droplet was moved to the right by applying a 34 Vrms and 1 kHz sine wave (V_{EWOD}) on the electrode highlighted by the dashed line. (d)–(f) Oil and water droplets were pumped for a complete loop. DEP and EWOD were determined by the applied signal and the manipulated droplets. (f), (g) The water droplet was driven by EWOD, while the oil droplet was stationary. (h) The water droplet merged with the oil droplet. (i) The water droplet moved in the oil by EWOD. (j)–(m) The merged water-in-oil droplet was driven by EWOD for a loop. (n)–(p) Separation of the merged water-in-oil droplet was achieved by DEP (solid line) and EWOD (dashed line) into water (mostly) and oil droplets. Some of the oil remained on the water droplet surface. The supplementary Video 2 ((b)–(e), concurrent oil and water droplet pumping), 3 ((f)–(m), merging droplets and transporting the merged droplet by EWOD), and 4 ((n)–(p), separating the merged droplet) can be seen in the ESI.†

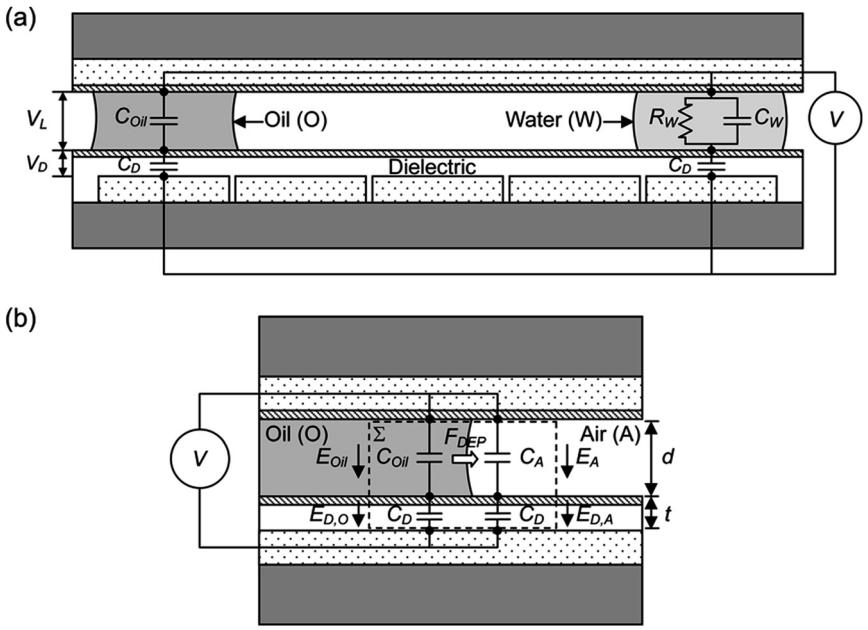

Fig. 4 Force analyses based on voltage distributions. (a) Simplified equivalent circuits of oil and water droplets. (b) A closed surface Σ at the oil meniscus used for Maxwell stress tensor evaluation of the DEP force.

the capacitor of the dielectric layer (C_D). From the simplified equivalent circuit of the water droplet (R_W in parallel with C_W), V_D would be dependent on the frequency of V applied between the parallel plates. At low frequencies, most V is consumed in the dielectric layer and generates EWOD. As the frequency increases, V_D decreases and V_L increases. The V_L at high frequencies has been applied to drive conductive liquids by DEP as mentioned above.[25,26] The frequency-dependent EWOD and DEP was discussed in literature.[23,24] We have also demonstrated a particle and cell concentrator by DEP on a EWOD device using different frequencies to obtain V_L or/and V_D.[29] In this platform, a 1 kHz sine wave signal was chosen to drive the water droplet by EWOD as our previous studies.[29] On the other hand, different from conductive droplets driven by dielectric-coated electrodes, the frequency of the applied signal does not influence the DEP force acting on the dielectric droplets because the ratio of the partial voltage distributed across two capacitors (*i.e.*, C_{Oil} and C_D) in series is not dependent on the frequency. As mentioned above, 1 kHz signals can also manipulate dielectric droplets by DEP, meaning 1 kHz signals would drive both dielectric and conductive droplets. However, because the required magnitudes of V_{DEP} and V_{EWOD} are quite different, a DC voltage was chosen to drive the oil droplet by DEP.

Although the supplemental dielectric layer is beneficial to EWOD, it reduces the DEP force F_{DEP} for the reduced V_L. F_{DEP} can be recalculated based on the closed surface (Σ, indicated by the dashed line in Fig. 4(b)) integral of the Maxwell stress tensor reported by Jones.[23,24] The derivation can be seen in the ESI,† and F_{DEP} with the supplemental dielectric layer is expressed as:

$$F_{DEP} = \frac{\varepsilon_0 \varepsilon_D W}{2} V^2 \left(\frac{\varepsilon_{Oil}}{\varepsilon_{Oil} t + \varepsilon_D d} - \frac{\varepsilon_{Air}}{\varepsilon_{Air} t + \varepsilon_{Oil} d} \right) \quad (2)$$

where ε_D, ε_{Oil}, and ε_{Air} are the relative permittivities of the dielectric layer, oil droplet, and air respectively, and t is the thickness of the dielectric layer. If t equals 0, eqn (2) is the same as eqn (1). F_{DEP} increases as d decreases, while the EWOD force, determined by the surface force, is theoretically independent of d. Therefore, the required voltages of DEP and EWOD may come closer by decreasing d, so that oil and water droplet would be driven by a single power source. Possible dielectric breakdown of the oil droplet caused by the decreased d should also be minded.

Conclusions

We successfully manipulated silicone oil droplets and dielectric organic solvent droplets, including decane and hexadecane, in parallel-plate devices by DEP. By supplementing a dielectric layer above the driving electrodes, DEP and EWOD were concurrently performed on a general digital microfluidic platform, where dielectric (silicone oil) and conductive (water) droplets were driven. Merging of water and oil droplets was performed. Transporting and splitting the merged water-in-oil droplet were demonstrated. The presented general digital microfluidic platform benefits LOC when regulating both dielectric and conductive droplets is necessary.

Acknowledgements

This work is partially supported by National Science Council, Taiwan, R.O.C. under grants NSC 95-2221-E-009-266-MY3, NSC 97-2627-M-009-004, and NSC 97-2218-E-006-004.

References

1 T. Taniguchi, T. Torii and T. Higuchi, *Lab Chip*, 2002, **2**, 19–23.
2 J. R. Millman, K. H. Bhatt, B. G. Prevo and O. D. Velev, *Nat. Mater.*, 2005, **4**, 98–102.
3 J. A. Schwartz, J. V. Vykoukal and P. R. C. Gascoyne, *Lab Chip*, 2004, **4**, 11–17.

4 S. K. Cho, H. Moon and C.-J. Kim, *J. Microelectromech. Syst.*, 2002, **12**, 70–80.
5 B. Berge and J. Peseux, *Eur. Phys. J. E*, 2000, **3**, 159–163.
6 S. Yang, T. N. Krupenkin, P. Mach and E. A. Chandross, *Adv. Mater.*, 2003, **15**, 940–943.
7 Z. Wan, H. Zeng and A. Feinerman, *Appl. Phys. Lett.*, 2006, **89**, 201107.
8 D. Y. Kim and A. J. Steckl, *Appl. Phys. Lett.*, 2007, **90**, 043507.
9 V. K. Pamula and K. Chakrabarty, *Proc. 13th ACM Great Lakes Symposium on VLSI*, Washington D.C., USA, 2003, 84–87.
10 J. Gong, G. Cha, Y. S. Ju and C.-J. Kim, *Proc. IEEE Conf. MEMS*, Tucson, Arizona, USA, 2008, 848–851.
11 H. Suzuki, K. Tabata, Y. Kato-Tamada, H. Noji and S. Takeuchi, *Lab Chip*, 2004, **4**, 502–505.
12 F. Mugele and J.-C. Baret, *J. Phys.: Comdens. Matter*, 2005, **17**, R705–R774.
13 D. Chatterjee, B. Hetayothin, A. R. Wheeler, D. J. King and R. L. Garrell, *Lab Chip*, 2006, **6**, 199–206.
14 H. A. Pohl, *Dielectrophoresis*, Cambridge University Press, New York, 1978.
15 K. D. Hermanson, S. O. Lumsdon, J. P. Williams, E. W. Kaler and O. D. Velev, *Science*, 2001, **294**, 1082–1086.
16 L. Zheng, J. P. Brody and P. J. Burke, *Biosens. Bioelectron.*, 2004, **20**, 606–619.
17 P. Y. Chiou, A. T. Ohta and M. C. Wu, *Nature*, 2005, **436**, 370–372.
18 O. D. Veleo, B. G. Prevo and K. H. Bhatt, *Nature*, 2003, **426**, 515–516.
19 H. Pellat, *C.R. Acad. Sci. Paris*, 1895, **119**, 691–694.
20 J. R. Melcher and M. Hurwitz, *J. Spacecr. Rockets*, 1967, **4**, 864–871.
21 J. R. Melcher, D. S. Guttman and M. Hurwitz, *J. Spacecr. Rockets*, 1969, **6**, 25–32.
22 J. R. Melcher, M. Hurwitz and R. G. Fax, *J. Spacecr. Rockets*, 1969, **6**, 961–967.
23 T. B. Jones, J. D. Fowler, Y. S. Chang and C.-J. Kim, *Langmuir*, 2003, **19**, 7646–7651.
24 K.-L. Wang and T. B. Jones, *J. Micromech. Microeng.*, 2004, **14**, 761–768.
25 T. B. Jones, *J. Electrost.*, 2001, **51–52**, 290–299.
26 R. Ahmed and T. B. Jones, *J. Micromech. Microeng.*, 2007, **17**, 1052–1058.
27 D. R. Lide, *CRC Handbook of Chemistry and Physics*, CRC Press, New York, 87th edn., 2006.
28 D. Brassard, L. Malic, F. Normandin, M. Tabrizian and T. Veres, *Lab Chip*, 2008, **8**, 1342–1349.
29 S.-K. Fan, P.-W. Huang, T.-T. Wang and Y.-H. Peng, *Lab Chip*, 2008, **8**, 1325–1331.